

A Study on the Retrofitting of the Shear Capacity on Cold Joint Longitudinal RC Beams

Ardi Azis Sila

Department of Civil Engineering, Faculty of Engineering, Universitas Hasanuddin, Indonesia
ardi.azis.sila@gmail.com (corresponding author)

Rita Irmawaty

Department of Civil Engineering, Faculty of Engineering, Universitas Hasanuddin, Indonesia
rita_irmawaty@yahoo.co.id (corresponding author)

Rudi Djamaluddin

Department of Civil Engineering, Faculty of Engineering, Universitas Hasanuddin, Indonesia
rudy0011@gmail.com

Wihardi Tjaronge

Department of Civil Engineering, Faculty of Engineering, Universitas Hasanuddin, Indonesia
tjaronge@yahoo.co.jp

Received: 5 August 2024 | Revised: 1 September 2024 | Accepted: 4 September 2024

Licensed under a CC-BY 4.0 license | Copyright (c) by the authors | DOI: <https://doi.org/10.48084/etasr.8622>

ABSTRACT

Strengthening of Reinforced Concrete (RC) beams using GFRP to increase flexural capacity often fails due to premature debonding and delamination of old concrete joints and grouting. The current research introduces a method of repairing and strengthening RC beams using grouting mortar, dyna-bold anchors, and Glass composite FRP (GFRP) sheets. Dyna-bold anchors are used as shear connectors between the old concrete and the grouting. In this research, 10 RC beams measuring 150 mm × 200 mm × 3300 mm, consisting of 2 control specimens (BK), 4 GFRP strengthening beams, and 4 GFRP strengthening beams with dyna-bolt anchors, were tested. The results show that the use of dyna-bold anchors in the joints between old concrete and grouting can increase the bending and shear capacity of the beam by 44.70%, indicating that the addition of dyna-bold anchors is able to prevent premature cracking along the joints and increase the stiffness and flexural capacity of the RC beams. These findings have significant practical implications for the repairing and strengthening of RC beams in real-world applications.

Keywords-RC-Beams; GFRP; spalling; retrofit; dyna-bold anchorage

I. INTRODUCTION

Concrete, a widely used construction material, is often combined with reinforcing steel to increase its performance. However, the presence of water and air contamination can cause carbonic acid to corrode steel or reinforcement, leading to spalling and affecting the performance of the concrete structure. Over time, various repair methods have been developed to repair or strengthen concrete due to spalling, with studies showing a significant influence on the strength of concrete after spalling [1-3].

Various strengthening methods have been developed over the last four decades [4], including externally bonded steel plates [5-6], Fiber-Reinforced Polymer (FRP) sheets [7], steel plates attached to the outside [8], concrete jacketing, and external weighting/beam strengthening techniques with external bars. When choosing the most appropriate method one

must consider the environmental conditions, the type of structure, repair costs, duration, and safety. FRP is a promising alternative for repairing damaged concrete elements with decreased strength. FRP sheets can practically bind or externally strengthen reinforced concrete slabs, beams, and columns [9]. GFRP sheets are applied externally by bonding to the concrete surface [10-12]. A recent study [13] proposed a new strengthening technique for corroded RC beams using Carbon Fiber Reinforced Polymer (CFRP) rods and anchor bolts, which increased the ultimate load capacity and maximum deflection of the RC beams up to 32.67% and 52%, respectively. CFRP is significantly more effective than GFRP in increasing the load capacity of RC beams that experience yield in their reinforcement [14-16]. A more effective and safer technique for strengthening RC beams is by using a combination of High-Performance Fiber Reinforced Cement-based Composite (HPFRCC) and CFRP [17]. Combining FRP

laminates and U-jackets can improve the flexural capacity and stiffness of RC beams damaged due to reinforcement corrosion [18, 19].

This research focuses on strengthening RC beams that experience spalling. Repairs were carried out with mortar grouting and the addition of dyna-bold anchors. GFRP was also added as a replacement for tensile and shear reinforcement in concrete beams to prevent premature delamination before it reaches its ultimate strength.



Fig. 1. Spalling of RC beams due to corrosion.

II. EXPERIMENTAL PROGRAM

A. Materials

Ready mix concrete was used with an average compressive strength of 23.48 MPa based on ASTM C39 [20], while the grouting mortar was prepared from Sikagrout 215 with an average compressive strength of 62.33 MPa as indicated in Table I. Table II displays the tensile test results of steel reinforcements (D10 mm for tensile reinforcement and $\phi 8$ mm for shear reinforcement).

TABLE I. COMPRESSIVE STRENGTH AT 28 DAYS

| Materials | Load (kN) | Section Area (mm ²) | Compressive strength (MPa) |
|-----------------|-----------|---------------------------------|----------------------------|
| Concrete | 184.43 | 7854 | 23.48 |
| Mortar Grouting | 489.56 | 7854 | 62.33 |

TABLE II. TENSILE STRENGTH OF REINFORCEMENTS

| Rebar | Diameters (mm) | Stress (MPa) | | Strain % |
|---------|----------------|--------------|----------|----------|
| | | Yield | Ultimate | |
| Tension | D10 | 430.95 | 620.82 | 25.25 |
| Stirrup | $\phi 8$ | 417.39 | 583.44 | 42.00 |

An adhesive from MAPEI was used, consisting of two components, resin (A), and a hardener (B) to fasten the GFRP sheet to a leveled and smooth concrete surface. The mix ratio of components A to B was 3:1. The GFRP applied is MapeWrap G UNI-AX type, with 2,560 MPa longitudinal tensile strength. Table III lists GFRP sheet characteristics and specifications [21].

Anchors played a vital role in connecting both structural and non-structural elements within the concrete. Their purpose

was to transfer external tensile and shear forces at the joints. In this investigation, M10 dyna-bold anchors with a post-installed system were utilized. This anchor is available in the local market. The post-installed anchorage system involved inserting anchors into the hardened concrete by drilling holes, ensuring efficient and convenient installation, as depicted in Figure 2.



Fig. 2. (a) Dyna-bold anchors, (b) installation.

TABLE III. SPECIFICATION OF GFRP MAPEI WRAP G TYPE OF DRY FABRIC

| Characteristics of MapeWrap G UNI-AX | |
|--------------------------------------|----------------------------|
| Property | Value |
| Density | 2.52 |
| Tensile strength | 2,560 MPa |
| Tensile strain | 3-4% |
| Mass | 900 g/m ² |
| Attachment to concrete | > 3 MPa (concrete rupture) |
| Modulus of elasticity | 80.7 GPa |

B. Test Specimens

In this research, a total of 10 RC beam specimens with dimensions of 150 mm x 200 mm x 3300 mm, consisting of 2 beams as control beams (BK), 2 monolith beams with GFRP (BNS), 2 beam specimens composite mortar grouting and GFRP (BGS), and 4 composite beams of mortar grouting, GFRP and added dyna-bold anchor shear connectors (BGSDB) (see Figure 3 for details). All beams utilized three deform bars for reinforcement: 3D10 mm for tensile and 2D10 for compression, except for BK beams which use 3D13 for tensile reinforcement. Meanwhile, $\phi 8$ -100/200 was used for shear reinforcement. The term monolith beam (BNS) refers to a normal RC beam filled with ready-mix concrete, where the tensile reinforcing area experienced a 41% reduction due to corrosion.

The process of making beam specimens starts with normal concrete casting and water curing until the age of 28 days, then continues with grouting mortar casting [22]. After 3 days, the compressive strength of the grouting mortar reached around 70% or higher of the compressive strength of the existing concrete and then the specimen could be tested. Especially for specimens with additional dyna-bold anchors, before the grouting mortar was cast, the dyna-bolds were first embedded into the old concrete at a depth of 6 cm using a hand drill. After all the concreting processes were complete, GFRP was installed on the bottom of the beam, which has been smoothed first with sandpaper.

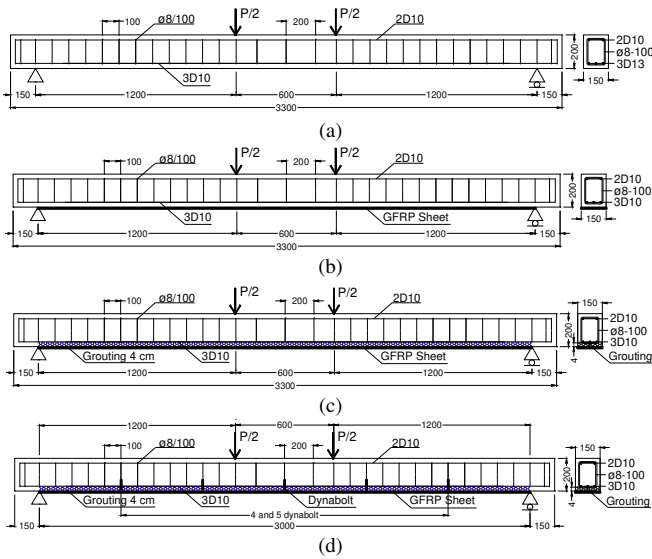


Fig. 3. Fig. 3 Detail specimens (a) control beam (BK), (b) beam with GFRP sheet (BNS), (c) beam composite grouting and GFRP sheet (BGS), (d) beam composite grouting, dyna-bolt anchors and GFRP sheet (BGSD4,5)

The process of making specimens in the laboratory is shown in Figure 4.



Fig. 4. Specimen preparation.

C. Test Setup

The bending test was performed after 28 days of placing the grouting mortar and ensuring complete bonding of GFRP. Bending tests at four points were given to the beam using a static loading machine with a capacity of 1500 kN. The beam was tested with a load that increased regularly by 0.2 mm/s at mid-span. The load was measured using a load cell with a capacity of 200 kN. To monitor deflection, three LVDT (Linear Variable Displacement Transducers) were installed at three points, namely in the mid-span and below the load points, as

shown in Figure 5. Each beam was fitted with a strain gauge to measure reinforcement, concrete, and GFRP strain. The strain gauges used in this study were FLK-2-11 for reinforcement, PL-60-11 for concrete, and FLA-6-11 for GFRP. Each strain gauge's position is on the material's surface, specifically in the middle part of the specimen's span as depicted in Figure 6.

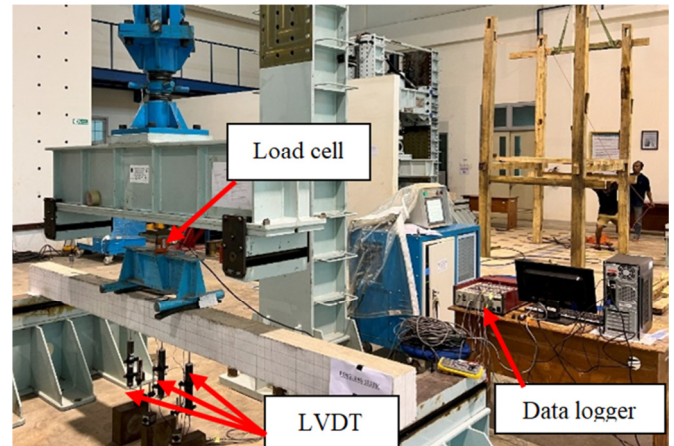


Fig. 5. Loading test.

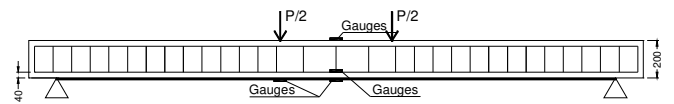


Fig. 6. Gauge positions.

III. RESULTS AND DISCUSSION

A. Load-Deflection at Midspan

Figure 7 shows the load-deflection relationship for all specimens, showing that, initially, all beams did not crack, indicating good concrete withstand ability. As the load increased, deflection increased slowly, and as the load reached maximum, the beams began to crack. The control beam (BK) experienced yielding when the load reached 16 kN, followed by the BGSD5, BGS, and BGSD4 beams at 21 kN, 22.1 kN, and 22.5 kN, respectively. The BNS beam achieved the highest yield load at 25.2 kN due to the monolith beam's action and the GFRP sheet's reinforcement. As the load increased, yielding occurred in the reinforcement, causing a decrease in flexural stiffness in all test specimens. The BGSD4 beam exhibited the greatest load and deflection among the beams, indicating a better adhesion effect between grouting mortar and old concrete at a certain dyna-bolt anchor distance.

This research focuses on post-spalling beam repair methods using grouting mortar, dyna-bolt anchors installed in old concrete-grouting mortar joints to prevent premature delamination, and strengthening with GFRP on the tensile side of the beam. The research results show that such repairs of the joints are proven to prevent premature delamination and debonding effectively compared to beams without dyna-bolt anchors. Several studies have been carried out, including the latest study by authors in [13] which proposed a new strengthening technique for corroding RC beams using CFRP

rods and anchor bolts. The analysis primarily focused on the final behavior to assess the strength gain produced by the CFRP anchored system. For the use of externally bonded steel plates to strengthen reinforced concrete structures, it is important to consider potential failure modes and prepare the concrete surface for bonding properly [7]. It is also important to ensure that the steel plate is compatible with the existing structure and consider the potential for premature debonding [8]. In some cases, it is also necessary to install additional steel rods or other structural reinforcement to support increased structural strength [23].

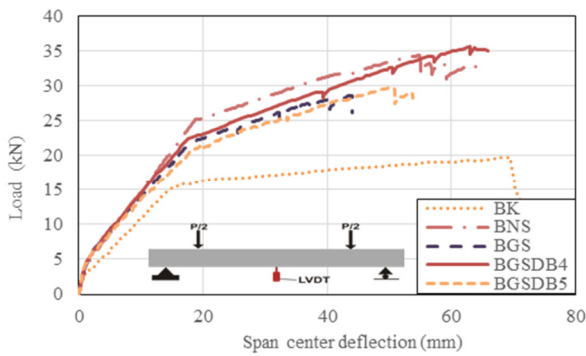


Fig. 7. Load-midspan deflection.

B. Ultimate Load

The impact of adding GFRP sheets to various beams is exhibited in Figure 8. The grouted mortar composite beam and GFRP sheet (BGS) showed a 31% increase in flexural capacity compared to the control beam (BK), while the monolith beam with GFRP (BNS) showed a 42.76% increase. The beam with additional dyna-bold anchors (BGSD5) also showed a 34.51% increase in bending load. However, the beam with 4 dyna-bold anchors (BGSD4) showed the highest flexural capacity (44.70%). The presence of dyna-bold anchors in the BGSD4 beam significantly increased the maximum load, resulting in a beam capacity exceeding the monolith beam (BNS) variation. This is due to the increased shear strength of old concrete joints with grouting mortar, thereby preventing premature delamination and cracking in the joint area.

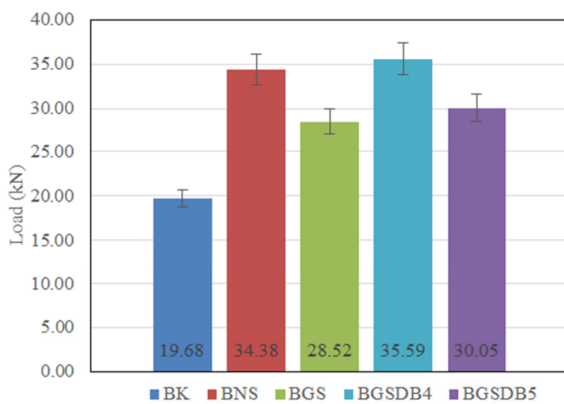


Fig. 8. Ultimate load.

C. Load-Concrete Strain Relationship

The load-strain relationship in concrete is illustrated in Figure 9, showing that no cracks occurred at the initiation of the loading test for all specimens. When the load approaches the maximum load, the strains at BK, BGSD4, BNS, BGSD5, and BGS were equal 0.0047, 0.0029, 0.0027, 0.0023, and 0.0017, respectively. The control beam BK has the highest ductility value, reaching an ultimate concrete strain of 0.003 before failure. The BGS beam has the lowest strain. Adding dyna-bold anchors to old and new concrete joints significantly increases the ultimate stiffness and strength of the BGSD4 beam by 6.62% to BNS and 41.29% compared to the beam without additional dyna-bold anchors (BGS).

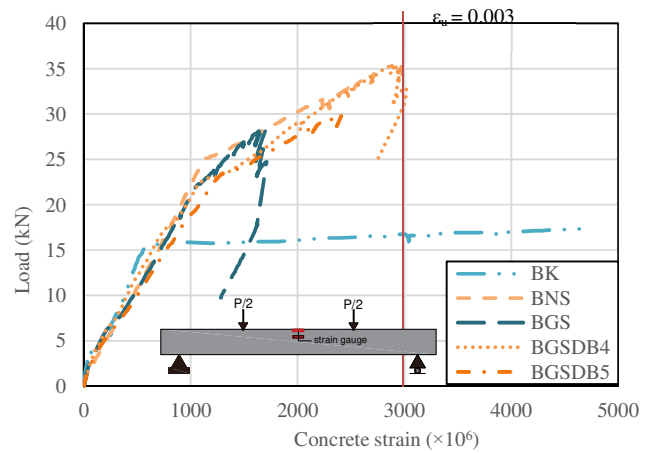


Fig. 9. Load-concrete strain.

D. Crack Pattern

1) Control Beam (BK)

The research design ensured that all RC beams experienced flexural failure, as demonstrated by the failure patterns of all specimens. The control beam (BK) exhibits a crack pattern with an initial crack on the tension side, propagating upwards towards the beam's neutral axis, as shown in Figure 10. The crack width at 20.13 kN was 2.5 mm.

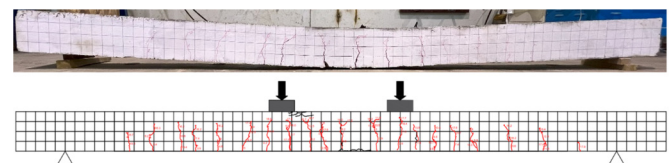


Fig. 10. Crack pattern of BK.

2) Beam with GFRP (BNS)

BNS or monolith beams without grouting mortar repairs that strengthened with additional GFRP sheets as a substitute for flexural reinforcement, resulting in higher maximum flexural strength and higher stiffness levels. Figure 11 shows that the crack that occurred was a vertical bending crack from the tensile side of the beam towards the neutral axis seen in the middle of the span, which propagated to the left and right

supports. A crack of 0.4 mm was observed in a BNS beam at 28.8 kN and increased to 3.6 mm at a load of 31.1 kN. The crack was followed by the debonding of the GFRP sheet towards the left support. When the load reached 32.8 kN, the concrete on the tensile side of the beam broke at 250 mm from the load support. Debonding continued to the support position of the left beam until the test was stopped.

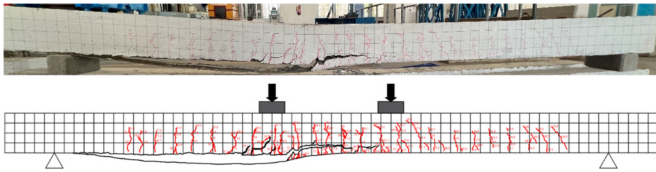


Fig. 11. Crack pattern of BNS

3) Beam with Grouting and GFRP (BGS)

Figure 12 displays the crack pattern observed in the BGS beam. During the initial loading, a vertical crack formed on the side of the material that was under tension, moving towards the neutral axis. At a load of 22.3 kN, the GFRP sheet experienced debonding, resulting in complete splitting and detachment on the left side of the beam. Additionally, horizontal cracks appeared at the old concrete joint with the grouting mortar, located just below the load support. The crack width was 0.4 mm to 0.8 mm when the force applied ranged from 24 kN to 27.3 kN. Concrete failure is characterized by the detachment (delamination) of the grouting mortar from the underlying concrete at the base of the support, which occurred when subjected to the maximum load of 28.5 kN.

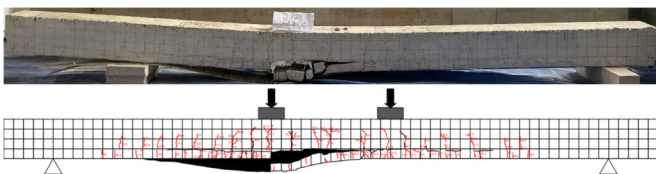


Fig. 12. Crack pattern of BGS.

4) Beam with Grouting, Dyna-bold, and GFRP (BGSDB4)

The BGSDB4 beam exhibited a crack pattern with an initial flexural crack occurring when the load reached 6.06 kN. Crack propagation occurred from the tension side to the compression side, exhibiting the same characteristics as the initial crack, as shown in Figure 13.

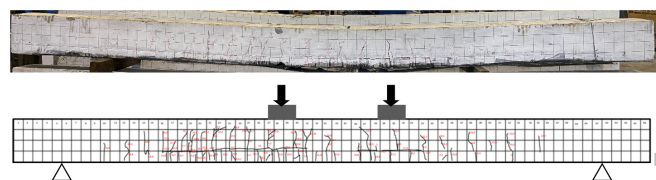


Fig. 13. Crack pattern of BGSDB4

Crack development was primarily caused by micro-cracks at the cold joint between the old concrete and the grouting

mortar, indicating the material's stiffness. The failure occurred due to local delamination in the connection at the midpoint of the span, where the highest moment occurred. Using dyna-bold anchors enhanced the beam's bending capacity, resulting in a maximum load-bearing capacity of 35.59 kN. It also effectively inhibited premature delamination in old concrete and grouting mortar joints.

5) Beam with Grouting, Dyna-bold, and GFRP (BGSDB5)

The BGS-DB beam's failure modes showed flexural failure, with cracks in old concrete joints and debonding of the GFRP sheet, as depicted in Figure 14. The crack width was measured as 0.8 mm at a peak load of 30 kN. Using dyna-bold anchors significantly enhanced the beam's overall strength compared to the BGS beam and prevented grouting mortar from separating from the existing concrete. The crack width was measured in the area where the crack was most extensive.

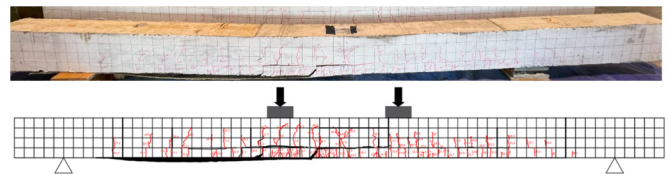


Fig. 14. Crack pattern of BGSDB5.

IV. CONCLUSIONS

After carrying out a series of experimental tests and thorough investigations on all specimens (BK beams, BNS beams, BGS beams, and BGS-DB beams with grouting mortar repairs, GFRP reinforcement, and additional dyna-bold anchors), the following conclusions can be drawn:

- Monolith beams with GFRP strengthening (BNS) show a 42.76% increase in flexural capacity compared to the un-strengthening beams (BK), while beams repaired with mortar grouting and GFRP reinforcement (BGS) have a 31% increase.
- The BGSDB5 beam, strengthened with mortar grouting, dyna-bold anchors, and GFRP sheet, showed a 34.51% increase in flexural capacity compared to the control beam, while the BGSDB4 beam achieved the highest strength (44.70% higher than BK).
- The crack pattern was flexural in all five beam variations. No horizontal cracks occurred on the BK beam. Four reinforced beams (BNS, BGS, BGSDB4, and BGSDB4) experienced horizontal cracks as the load increased. Delamination failure occurred in BGS and BGSDB beams, causing concrete expansion and GFRP debonding.
- The dyna-bold anchors in BGSDB4 beams provided superior performance. This indicated that dyna-bold anchors contribute to the shear strength of old concrete connections with mortar grouting increasing the flexural capacity.

The results of this study show that using 4 and 5 dyna-bold anchors results in a significant increase in beam capacity; however, variations in the number and distance of the anchors

may require further studies to determine the optimum number and distance for increasing beam capacity.

REFERENCES

- [1] L. Wang, X. Zhang, J. Zhang, Y. Ma, Y. Xiang, and Y. Liu, "Effect of insufficient grouting and strand corrosion on flexural behavior of PC beams," *Construction and Building Materials*, vol. 53, pp. 213–224, Feb. 2014, <https://doi.org/10.1016/j.conbuildmat.2013.11.069>.
- [2] F. Moccia, M. Fernández Ruiz, and A. Muttoni, "Spalling of concrete cover induced by reinforcement," *Engineering Structures*, vol. 237, Jun. 2021, Art. no. 112188, <https://doi.org/10.1016/j.engstruct.2021.112188>.
- [3] D. Qiao, H. Nakamura, K. K. Tran, Y. Yamamoto, and T. Miura, "Experimental and analytical evaluation of concrete cover spalling behavior due to local corrosion," *Journal of Structural Engineering*, vol. 61A, pp. 707–714, 2015, <https://doi.org/10.11532/structcivil.61A.707>.
- [4] P. Ganesh and A. R. Murthy, "Repair, retrofitting and rehabilitation techniques for strengthening of reinforced concrete beams - A review," *Advances in Concrete Construction*, vol. 8, no. 2, pp. 101–117, Oct. 2019, <https://doi.org/10.12989/ACC.2019.8.2.101>.
- [5] E. Ciampa, F. Ceroni, and M. R. Pecce, "Bond Behavior of Steel Plates Externally Bonded on Concrete Elements," in *10th International Conference on FRP Composites in Civil Engineering*, Istanbul, Turkey, Dec. 2021, pp. 232–242, https://doi.org/10.1007/978-3-030-88166-5_19.
- [6] M. Z. Jumaat and M. A. Alam, "Strengthening of R.C. beams using externally bonded plates and anchorages," *Australian Journal of Basic and Applied Sciences*, vol. 3, no. 3, pp. 2207–2211, 2009.
- [7] H.-T. Wang and G. Wu, "Bond-slip models for CFRP plates externally bonded to steel substrates," *Composite Structures*, vol. 184, pp. 1204–1214, Jan. 2018, <https://doi.org/10.1016/j.compstruct.2017.10.033>.
- [8] A. S. Alshaiikhly, Md. A. Alam, and K. N. Mustapha, "An Advanced Method for Repairing Severely Damaged Beams in Shear with Externally Bonded Steel Plates Using Adhesive and Steel Connectors," *Arabian Journal for Science and Engineering*, vol. 41, no. 10, pp. 4077–4097, Oct. 2016, <https://doi.org/10.1007/s13369-016-2079-5>.
- [9] *ACI440R-96(1996), Report on Fiber Reinforced Plastic Reinforcement for Concrete Structures*. Farmington Hills, MI, USA: ACI Concrete, 1996.
- [10] R. Djamaluddin, Hijriah, R. Irmawati, Faharuddin, and R. T. Wahyuningsih, "Delamination mechanism of GFRP sheet bonded on the reinforced concrete beams," *MATEC Web of Conferences*, vol. 258, 2019, Art. no. 03009, <https://doi.org/10.1051/mateconf/201925803009>.
- [11] T. H. Almusallam, "Load-deflection behavior of RC beams strengthened with GFRP sheets subjected to different environmental conditions," *Cement and Concrete Composites*, vol. 28, no. 10, pp. 879–889, Nov. 2006, <https://doi.org/10.1016/j.cemconcomp.2006.07.017>.
- [12] R. Djamaluddin, R. Irmawaty, and A. Tata, "Flexural Capacity of Reinforced Concrete Beams Strengthened Using GFRP Sheet after Fatigue Loading for Sustainable Construction," *Key Engineering Materials*, vol. 692, pp. 66–73, 2016, <https://doi.org/10.4028/www.scientific.net/KEM.692.66>.
- [13] H. A. Y. Al-Mashgari, F. Hejazi, and M. Y. Alkhateeb, "Retrofitting of corroded reinforced concrete beams in flexure using CFRP rods and anchor bolt," *Structures*, vol. 29, pp. 1819–1827, Feb. 2021, <https://doi.org/10.1016/j.istruc.2020.12.047>.
- [14] H. Machmud, M. W. Tjaronge, R. Djamaluddin, and D. R. Irmawaty, "The capacity of reinforced concrete beams post rebars yielded with Frp sheet strengthening," *International Journal of Civil Engineering and Technology*, vol. 10, no. 9, pp. 232–241, 2019.
- [15] T. Do-Dai, T. Chu-Van, D. T. Tran, A. Y. Nassif, and L. Nguyen-Minh, "Efficacy of CFRP/BFRP laminates in flexurally strengthening of concrete beams with corroded reinforcement," *Journal of Building Engineering*, vol. 53, Aug. 2022, Art. no. 104606, <https://doi.org/10.1016/j.jobe.2022.104606>.
- [16] R. Irmawaty, Fakhruddin, and J. J. Ekaputri, "Experimental and analytical study for shear strengthening of reinforced-concrete beams using a prefabricated geopolymer–mortar panel," *Case Studies in Construction Materials*, vol. 17, Dec. 2022, Art. no. e01568, <https://doi.org/10.1016/j.cscm.2022.e01568>.
- [17] V. J. Ferrari, J. B. de Hanai, and R. A. de Souza, "Flexural strengthening of reinforcement concrete beams using high performance fiber reinforcement cement-based composite (HPFRCC) and carbon fiber reinforced polymers (CFRP)," *Construction and Building Materials*, vol. 48, pp. 485–498, Nov. 2013, <https://doi.org/10.1016/j.conbuildmat.2013.07.026>.
- [18] T. H. Ibrahim, I. A. S. Alshaarbaf, A. A. Allawi, N. K. Oukaili, A. El-Zohairy, and A. I. Said, "Theoretical Analysis of Composite RC Beams with Pultruded GFRP Beams subjected to Impact Loading," *Engineering, Technology & Applied Science Research*, vol. 13, no. 6, pp. 12097–12107, Dec. 2023, <https://doi.org/10.48084/etasr.6424>.
- [19] J. Yang, R. Haghani, T. Blanksvärd, and K. Lundgren, "Experimental study of FRP-strengthened concrete beams with corroded reinforcement," *Construction and Building Materials*, vol. 301, Sep. 2021, Art. no. 124076, <https://doi.org/10.1016/j.conbuildmat.2021.124076>.
- [20] *ASTM C39/C39M-18(2018), Standard Test Method For Compressive Strength Of Cylindrical Concrete Specimens*. West Conshohocken, PA, USA: ASTM International, 2018.
- [21] "Mapei - adhesives, sealants, chemical products for building," *GlobalLanding*. <https://www.mapei.com>.
- [22] *ASTM C33/C33M-16(2016), Standard Specification For Concrete Aggregates*. West Conshohocken, PA, USA: ASTM International, 2016.
- [23] E. Julio, F. A. B. Branco, and V. D. Silva, "Reinforced concrete jacketing-interface influence on monotonic loading response," *ACI Structural Journal*, vol. 102, no. 2, pp. 252–257, Mar. 2005.